



OPEN

# Functional and Structural Integrity of Frontoparietal Connectivity in Traumatic and Anoxic Coma

Patrice Peran, PhD<sup>1</sup>; Briguitta Malagurski, PhD<sup>1</sup>; Federico Nemmi, PhD<sup>1</sup>; Benjamine Sarton, MD<sup>1,2</sup>; Hélène Vinour, MD<sup>2</sup>; Fabrice Ferre, MD<sup>1,2</sup>; Fanny Bounes, MD<sup>3</sup>; David Rousset, MD<sup>4</sup>; Segolène Mrozeck, MD, PhD<sup>4</sup>; Thierry Seguin, MD<sup>3</sup>; Béatrice Riu, MD<sup>2</sup>; Vincent Minville, MD, PhD<sup>5</sup>; Thomas Geeraerts, MD, PhD<sup>4</sup>; Jean Albert Lotterie, MD, PhD<sup>1</sup>; Xavier Deboissezon, MD, PhD<sup>1,6</sup>; Jean François Albucher, MD<sup>1,7</sup>; Olivier Fourcade, MD, PhD<sup>4</sup>; Jean Marc Olivot, MD, PhD<sup>1,7</sup>; Lionel Naccache, MD, PhD<sup>8</sup>; Stein Silva, MD, PhD<sup>1,2</sup>

**Objectives:** Recovery from coma might critically depend on the structural and functional integrity of frontoparietal networks. We aimed to measure this integrity in traumatic brain injury and anoxic-ischemic (cardiac arrest) coma patients by using an original multimodal MRI protocol.

**Design:** Prospective cohort study.

**Setting:** Three Intensive Critical Care Units affiliated to the University in Toulouse (France).

**Patients:** We longitudinally recruited 43 coma patients (Glasgow Coma Scale at the admission < 8; 29 cardiac arrest and 14 traumatic brain injury) and 34 age-matched healthy volunteers. Exclusion criteria were disorders of consciousness lasting more than 30 days and focal brain damage within the explored brain regions. Patient assessments were conducted at least 2 days (5 ± 2 d)

after complete withdrawal of sedation. All patients were followed up (Coma Recovery Scale-Revised) 3 months after acute brain injury.

**Interventions:** None.

**Measurements and Main Results:** Functional and structural MRI data were recorded, and the analysis was targeted on the posteromedial cortex, the medial prefrontal cortex, and the cingulum. Univariate analyses and machine learning techniques were used to assess diagnostic and predictive values. Coma patients displayed significantly lower medial prefrontal cortex–posteromedial cortex functional connectivity (area under the curve, 0.94; 95% CI, 0.93–0.95). Cardiac arrest patients showed specific structural disturbances within posteromedial cortex. Significant cingulum architectural disturbances were observed in traumatic brain injury patients. The machine learning medial prefrontal cortex–posteromedial cortex multimodal classifier had a significant predictive value (area under the curve, 0.96; 95% CI, 0.95–0.97), best combination of subregions that discriminates a binary outcome based on Coma Recovery Scale-Revised).

**Conclusions:** This exploratory study suggests that frontoparietal functional disconnections are specifically observed in coma and their structural counterpart provides information about brain injury mechanisms. Multimodal MRI biomarkers of frontoparietal disconnection predict 3-month outcome in our sample. These findings suggest that fronto-parietal disconnection might be particularly relevant for coma outcome prediction and could inspire innovative precision medicine approaches. (*Crit Care Med* 2020; 48:e639–e647)

**Key Words:** brain anoxia; brain trauma; coma; functional magnetic resonance imaging; prognosis

<sup>1</sup>Toulouse Neuroimaging Center, Toulouse University, Inserm, UPS, Toulouse, France.

<sup>2</sup>Critical Care Unit, University Teaching Hospital of Purpan, Place du Dr Baylac, Toulouse, France.

<sup>3</sup>Critical Care Unit, University Teaching Hospital of Rangueil, Avenue Pr Jean Poulhès, Toulouse, France.

<sup>4</sup>Neurocritical Care Unit, University Teaching Hospital of Purpan, Place du Dr Baylac, Toulouse, France.

<sup>5</sup>Anesthesiology Department, University Teaching Hospital of Purpan, Place du Dr Baylac, Toulouse, France.

<sup>6</sup>Physical Medicine and Rehabilitation Department, University Teaching Hospital of Purpan, Place du Dr Baylac, Toulouse, France.

<sup>7</sup>Neurology Department, University Teaching Hospital of Purpan, Place du Dr Baylac, Toulouse, France.

<sup>8</sup>Institut du Cerveau et de la Moelle épinière, ICM, PICNIC Lab, Paris, France.

Copyright © 2020 The Author(s). Published by Wolters Kluwer Health, Inc. on behalf of the Society of Critical Care Medicine and Wolters Kluwer Health, Inc. This is an open-access article distributed under the terms of the Creative Commons Attribution-Non Commercial-No Derivatives License 4.0 (CCBY-NC-ND), where it is permissible to download and share the work provided it is properly cited. The work cannot be changed in any way or used commercially without permission from the journal.

DOI: 10.1097/CCM.0000000000004406

It has been suggested that problems to efficiently transfer neuroscience from bench to bedside in the clinical setting of coma are related to an incomplete description of

structural and functional brain damages associated to severe brain injury (1). A growing body of literature (2) support the idea that state-of-the-art neuroimaging methods have potential to fill this knowledge gap. However, these studies have some limitations: 1) most of the patients enrolled were suffering with chronic disorders of consciousness (DoC) (i.e., vegetative state [VS]/unresponsive wakefulness syndrome [UWS], and minimally conscious state [MCS]) (3–13), and only few were evaluated during the acute phase of DoC corresponding to coma (14–17); 2) the vast majority of these studies have gathered neuroimaging data almost entirely disregarding DoC etiologies; and 3) the clear majority of the reported studies have used neuroimaging techniques in isolation and have not compared structural and functional data, despite the fact that the relationships between structural and functional brain connectivity might not be straightforward (18).

Connectivist theoretical frameworks for conscious access (19) support the hypothesis of a “global neural workspace” (19), encompassing frontal (medial prefrontal cortex [mPFC]) and parietal (posteromedial cortex [PMC]) structures, as a plausible candidate for the neural bases of consciousness. Indeed, a selective hypometabolism in these two cortical structures has been reported in a wide range of altered conscious states such sleep (20), drug-induced anesthesia (21), or acquired chronic DoC states (13, 15). In the specific case of coma, frontoparietal functional disconnection have been recently reported (22–24). Interestingly, the strength of mPFC–PMC functional connectivity (FC) seems to differ between coma patients who recover and those who eventually score an unfavorable outcome at 3 months (15). The mechanism underpinning this critical functional frontoparietal disconnection is not well understood. It has been suggested that coma related PMC–mPFC functional disconnection might be due either to disruptions of the cingulum, the bundle of white matter fibers that directly relies PMC to mPFC (i.e., cingulum) (6), and/or to gray matter (GM) structural disturbances within these regions (16). To the extent of our knowledge, there is not study providing a complete and comprehensive assessment of this key frontoparietal connection in coma, despite the significant value that may have such information for the development of news tools for coma patient’s neurologic prognostication.

In the present work, we aimed at measuring the residual integrity of mPFC–PMC brain structure-FC in a cohort of mixed-cases of coma patients by using a data-driven combination of advanced structural (mPFC and PMC GM integrity; cingulum microarchitecture) and functional (resting-state FC between mPFC and PMC explored at level of whole regions and subregions) MRI metrics. We hypothesize that: 1) mPFC–PMC functional disconnections are, regardless of its etiology, reliable biomarkers of coma; 2) mechanisms of coma have specific structural signatures, both in terms of GM and white matter (WM) anomalies; and 3) combined functional and structural markers of disconnection between mPFC and PMC, may help predicting coma patient’s 3 months outcome. We conducted a prospective study using neuroimaging on both traumatic and anoxo-ischemic coma patients to increase

the generalizability of our findings. Patients were managed by treating teams blinded to multimodal imaging data and were scanned during the acute phase following the primary brain insult, exclusively during coma. The prognostic value of neuroimaging data were assessed against neurologic outcome using a validated behavioral score (25), 3 months after the primary brain injury.

## MATERIALS AND METHODS

### Participants

This prospective study was undertaken in three ICUs affiliated with the University Hospital (Toulouse, France), between January 2015 and December 2017. Patients were included in the study after they had a behavioral assessment with Glasgow Coma Scale (GCS) and had been diagnosed as been in coma (GCS score at the admission to hospital  $\leq 6$  with motor responses  $< 6$ ) induced by a severe traumatic or anoxo-ischemic (i.e., cardiac arrest) brain injury. Exclusions criteria were as follows: DoC state lasting more than 30 days after primary brain injury; focal brain damage within the cortical or subcortical explored brain regions (i.e., frontal and posteroparietal cortices; cingulum) as stated by a certified neurologist using T1 and fluid-attenuated inversion recovery MRI sequences; and motion of more than 3 mm in translation and  $3^\circ$  in rotation during functional MRI (fMRI) acquisition. Patients were managed according to standard of care recommendations (26, 27) by physicians blinded to neuroimaging data. To avoid confounding factors, all patient assessments were conducted at least 2 days ( $4 \pm 2$  d) after complete withdrawal of sedative drug therapy and were performed under normothermic conditions. In patients, standardized clinical examination was performed by raters blinded to neuroimaging data (GCS [28] and the Full Outline of UnResponsiveness [29])—on the day of patients’ admission to the hospital, the day of scanning and 3 mo after the primary brain injury by using the Coma Recovery Scale-Revised [CRS-R] [25]). Over the same recruitment period, 34 controls, matched by age, were recruited and included if they had normal neurologic examination results and no history of neurologic or psychiatric disorder. Our study was approved by the Ethics Committee of the University Teaching Hospital of Toulouse, France. Informed and written consent to participate to the study was obtained from the subjects themselves in the case of healthy subjects and from legal surrogate of the patients. Clinical trials identifiers: NCT01620957 and NCT03482115.

### Data Acquisition

In all participants, 11 minutes of resting-state fMRI (rs-fMRI) was acquired on the same 3T magnetic resonance scanner (Intera Achieva; Philips, Best, The Netherlands). High-resolution anatomical image, using 3D T1-weighted sequence and diffusion tensor imaging (DTI) were also acquired (Text-e1, Supplemental Digital Content 1, <http://links.lww.com/CCM/F502>). Monitoring of vital measures was performed by a senior intensivist throughout the experiment.

## Data Processing

**Structural Brain Markers.** GM morphometry was applied on 3D T1-weighted images by using voxel-based morphometry. To assess WM integrity, DTI models were created to fit at each voxel, generating fractional anisotropy (FA), mean diffusivity (MD), and radial diffusivity (RD) maps (30). Cortical (PMC and mPFC) and subcortical (cingulum) regions of interest (ROI) were defined (Fig. 1). To assess GM changes, we extracted the mean values of GM density (GMD) and MD from 11 mPFC subregions and three PMC subregions, which were defined according to fMRI segmentation. The cingulum was divided into five subregions equally distributed along an anteroposterior axis (Fig. 1; and Text-e1, Supplemental Digital Content 1, <http://links.lww.com/CCM/F502>).

**Functional Brain Markers.** rs-fMRI data was preprocessed using Statistical Parametric Mapping (Version SPM 12, Wellcome Trust Center for Neuroscience, London, United Kingdom; <http://www.fil.ion.ucl.ac.uk/spm/>). The fMRI images were realigned, slice-time corrected, coregistered to each subject's

T1-weighted image, and normalized to standard stereotaxic anatomical Montreal Neurologic Institute space. We targeted our analysis on three subregions of the PMC, and 11 subregions of the mPFC, as described in functional atlas (Fig. 1).

## Statistical Analysis

The mean values of GMD, MD, FA, and FC were compared using a repeated-measures multivariate analysis of variance with two factors (group, subregion). In case of significant results (group effect or group by subregion interaction), a one-way analysis of variance with group as factor was applied to each parameter and each structure. We also performed a “whole-region” analyses averaging the values in the subregions for mPFC, PMC, and the cingulum (Text-e2, Supplemental Digital Content 2, <http://links.lww.com/CCM/F503>). To complement these univariate analyses, we have performed discriminative and predictive analyses using machine learning techniques.

**Single Markers and Two Markers Combination.** First, we wanted to test the hypothesis that single MRI indexes in

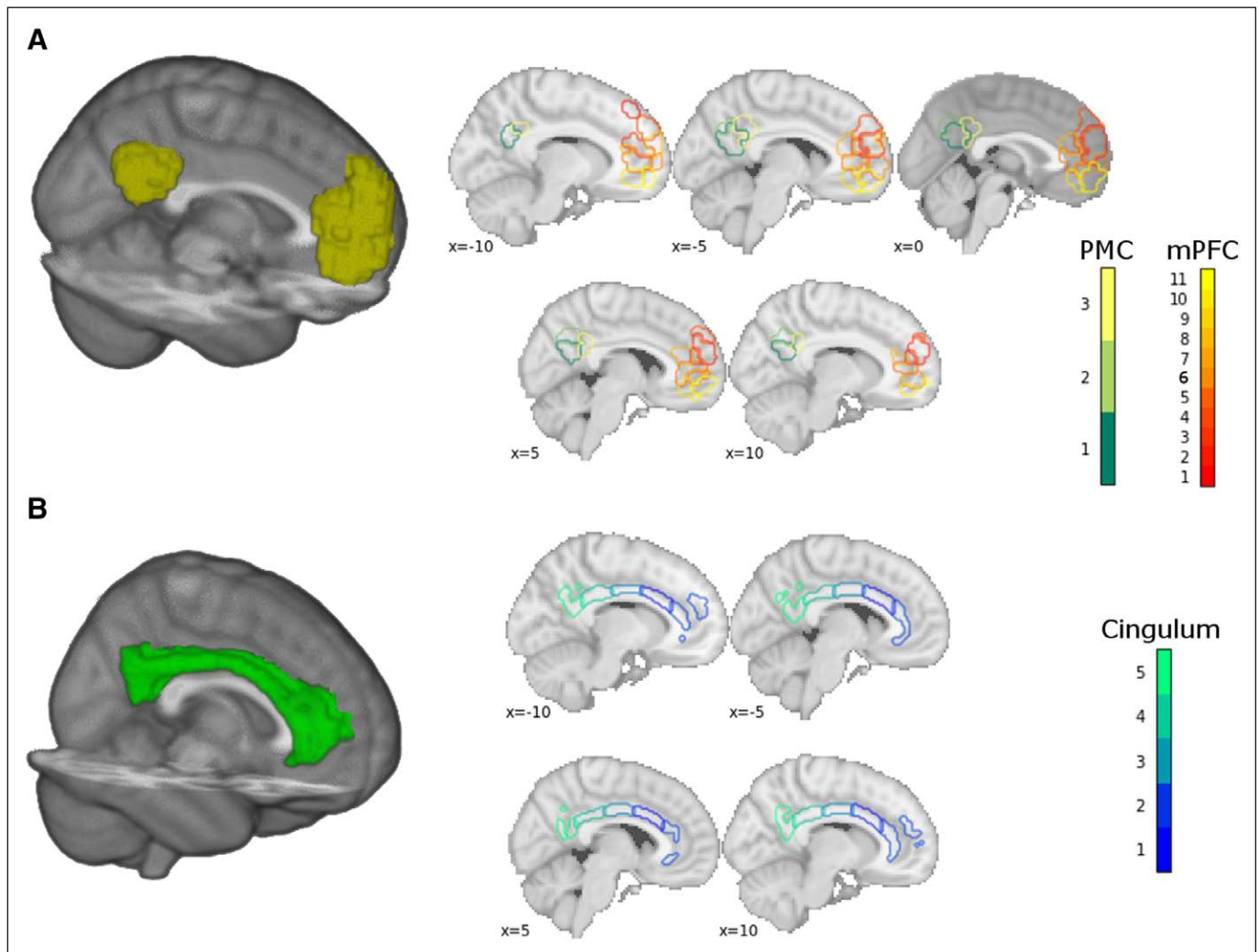


**Figure 1.** Functional and structural regions of interests (ROIs). **A**, Medial prefrontal cortex (mPFC) and posteromedial cortex (PMC). *Leftmost* shows a 3D rendering of the whole mPFC and PMC ROIs. *Rightmost* shows the outline of the 11 mPFC subregions and the three PMC subregions from the Willard atlas on a standard T1 template. **B**, Cingulum. *Leftmost* shows a 3D rendering of the whole cingulum as defined (10). *Rightmost* shows the outline of the five cingulum subregions (see methods).



isolation could discriminate between healthy controls and patients in coma, between traumatic brain injury (TBI) and anoxic patients as well as predict the clinical outcome measured 3 months after the MRI acquisition. Furthermore, we were interested in testing the discriminative and predictive power of canonical anatomical ROIs. We extracted the FC between mPFC and the PMC, the GM volume from the mPFC and the PMC, and the MD, RD and FA from the PFC, the PMC, and the cingulum. We also used more spatially specific ROIs that subdivide the structures of interest in functional/anatomical units to test the hypothesis that increased spatial specificity could improve the discriminative/predictive performance. As for outcome variables, we used the following variables: coma patients versus healthy controls (binary), TBI versus anoxic patient (binary), recovered (MCS—encompassing both MCS [–] and MCS [+]) (which were defined according to the identification of command-following, intelligible verbalization or intentional communication abilities) (31–33) versus nonrecovered (VS/UWS) patients (binary) and CRS-R (continuous variable). We used logistic regression without penalty for binary variables and linear regression for continuous ones, using a repeated (1,000 times) 10-fold cross-validation approach to ensure unbiased prediction (Text-e1, Supplemental Digital Content 1, <http://links.lww.com/CCM/F502>).

**Predictive Models With All Indexes and Regions.** To confirm the discriminative and predictive power of the different markers/regions, we also ran analyses using all markers and regions at the same time, while recording the performance of the models and the number of times a certain marker/region were selected. We combined a supporting vector machine (SVM, linear support vector classification for binary variables and linear support vector regression for continuous variables, in the scikit-learn implementation, with default hyperparameters –L1 penalty,  $C = 1$  for classification;  $\epsilon = 0.1$ ,  $C = 1$  for regression) with a univariate filter for features selection. SVM was chosen due to its robustness to small sample size. As for the univariate filter, we used an F-score filter to only retain the  $k$  features with the highest association with the outcome variables before fitting the model. The parameter  $k$  (i.e., the proportion of features to retain, set to be [0.9, 0.8, 0.7, 0.6, 0.5, 0.4, 0.3, 0.2, 0.1]) was selected using a 10-fold cross-validation scheme nested into a bootstrap procedure. Note that the performance of the models was evaluated using out-of-bag methods (i.e., using the subjects that were not resampled in the bootstrap procedures as testing set at each iteration) to obtain unbiased prediction. We repeated the bootstrap procedure 1,000 times and calculated the mean and 95% CI of the performance of the model (balanced accuracy for the binary variables, correlation between the predictions and the actual value as well as absolute mean error [ame] for the continuous variables). We used permutations to assess statistical significance. The entire procedure was repeated shuffling the labels/outcomes of the subjects in order to obtain an approximation of the null distribution of performances (i.e., the distribution of performances when there is no association between features and label/outcome). To test the significance of the performance

obtained with the original labels/outcome we counted the number of times a model fitted with shuffled labels reached an accuracy equal or higher than the median of the performance obtained with the true labels and divided this number by the total number of shuffling (i.e., 1,000). To test the robustness of our model to different validation methods, we have performed a similar analysis using a nested repeated 10-fold cross-validation scheme obtaining similar results (Text-e1, Supplemental Digital Content 1, <http://links.lww.com/CCM/F502>).

## RESULTS

### Population

Between January 1, 2015, and December 31, 2017, 47 patients were enrolled in our study. Three were excluded because of excessive motion during MRI acquisition and one was excluded due to failure of brain images normalization process. Therefore, we compared 43 patients with severe brain injury who met the clinical definition of coma (GCS score at the admission to hospital  $< 6$  with motor responses  $< 6$ ; 14 patients with traumatic and 29 with anoxic brain injury; age range, 21–76 and 22–78, respectively) with 34 age-matched healthy volunteers (range, 22–74 yr). The delay from coma onset to imaging was 6 days ( $6 \pm 3$  d). Table-e1 (Supplemental Digital Content 3, <http://links.lww.com/CCM/F504>) reports patient's demographics and clinical characteristics.

### Neural Signatures of Coma

Comatose patients displayed significantly lower mPFC–PMC FC values, both in subregions (Fig. 2; and Table-e2, Supplemental Digital Content 4, <http://links.lww.com/CCM/F505>) and whole-region (Fig.-e1, Supplemental Digital Content 5, <http://links.lww.com/CCM/F506> [legend, Supplemental Digital Content 8, <http://links.lww.com/CCM/F509>]; and Text-e2, Supplemental Digital Content 2, <http://links.lww.com/CCM/F503>) analyses. The average mPFC–PMC connectivity reached an area under the curve (AUC) of 0.94 (95% CI, 0.93–0.95) (the second best marker was the MD in cingulum with a mean AUC of 0.65). The best combination of two markers reached the same AUC of 0.94 (95% CI, 0.93–0.95) (combination of mPFC–PMC connectivity with the average MD in the cingulum) (Fig.-e2, Supplemental Digital Content 6, <http://links.lww.com/CCM/F507>; legend, Supplemental Digital Content 8, <http://links.lww.com/CCM/F509>). The subregions leading to the best performance and the decision surface of the model are shown in Figure-e2 (Supplemental Digital Content 6, <http://links.lww.com/CCM/F507>; legend, Supplemental Digital Content 8, <http://links.lww.com/CCM/F509>). Entering all indexes in a pipeline combining univariate features selection and SVC resulted in a mean accuracy of 0.83 for group discrimination ( $p = 0.006$ ; false discovery rate [FDR]- $p = 0.008$ ). The most frequently selected features were those relative to mPFC–PMC subregions FC, with the connectivity between mPFC02 and PMC02 as well as between mPMC02 and PMC03 selected in almost all the repetitions.

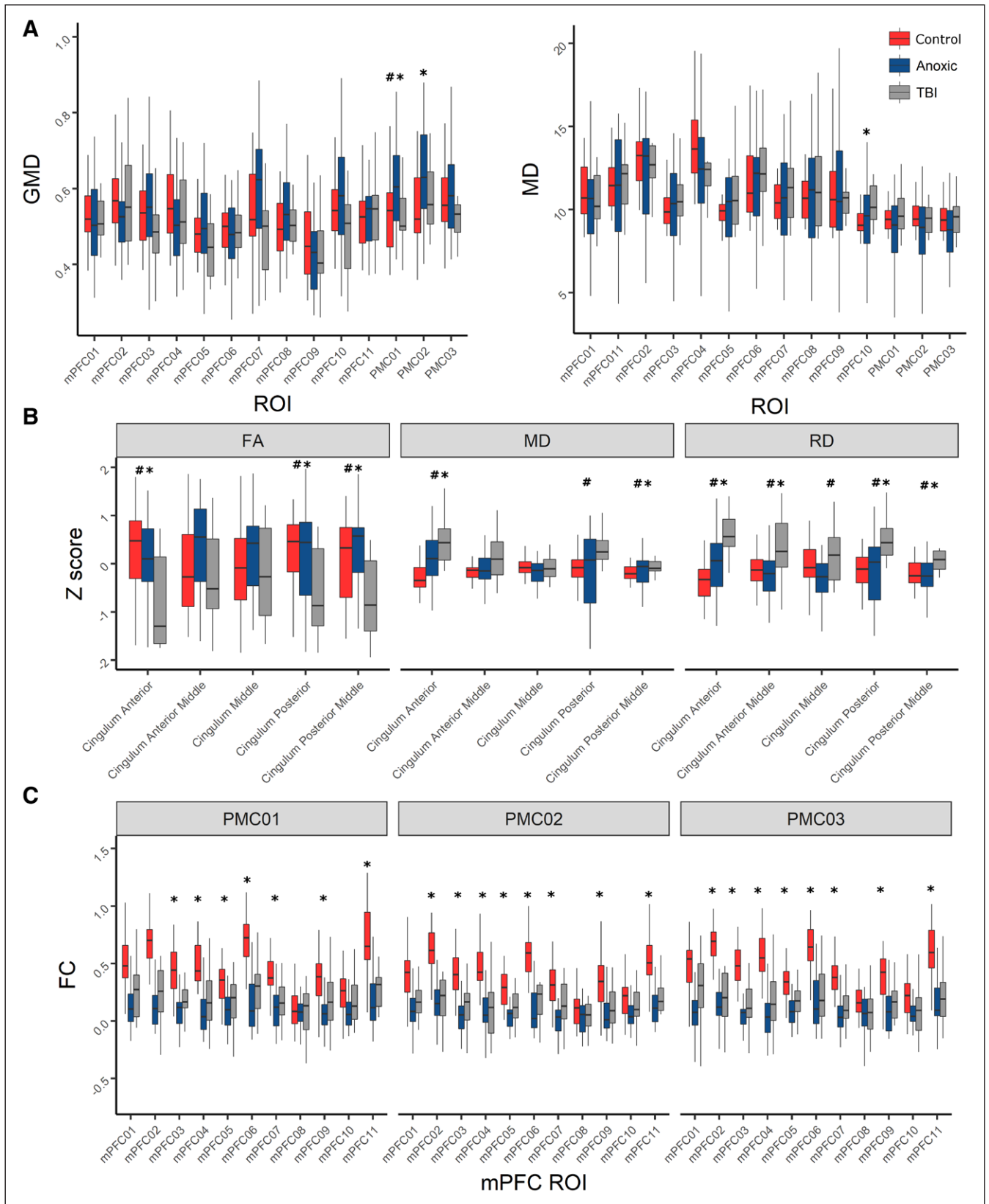


**Figure 2.** Univariate analysis of regions of interests (ROIs) subregions. **A**, Cortex: *boxplot* of the two indexes pertaining to the cortex, gray matter density (GMD) and mean diffusivity (MD), broken down by medial prefrontal cortex (mPFC) and posteromedial cortex (PMC) subregions. MD values were multiplied by a constant for easiness of visualization and comparison with GMD values. **B**, Cingulum: *boxplot* of the three indexes pertaining to the cingulum, fractional anisotropy (FA), MD, and radial diffusivity (RD) broken down by mPFC and PMC subregions. FA, MD, and RD values were Z transformed for easiness of visualization and comparisons between indexes. **C**, Functional connectivity (FC) (measured as Fisher-transformed Pearson  $r$ ) between the mPFC and PMC subregions. \*Significant diagnosis effect (healthy controls vs coma); #Significant etiology effect (traumatic brain injury [TBI] vs anoxic).

### Brain Injury Mechanisms

There was no relationship between coma mechanism and functional markers (Fig. 2; Fig.-e1, Supplemental Digital Content 5, <http://links.lww.com/CCM/F506> [legend, Supplemental Digital Content 8, <http://links.lww.com/CCM/F509>]; and Table-e2, Supplemental Digital Content 4, <http://links.lww.com/CCM/F505>). Nevertheless, anoxo-ischemic patients showed significantly higher GMD than controls and traumatic patients within PMC (Fig. 2; Fig.-e1, Supplemental Digital Content 5, <http://links.lww.com/CCM/F506> [legend, Supplemental Digital Content 8, <http://links.lww.com/CCM/F509>]; and **Table e-3**, Supplemental Digital Content 7, <http://links.lww.com/CCM/F508>). Furthermore, structural markers derived from the cingulum analysis, enabled to accurately distinguish traumatic patients from controls and anoxo-ischemic groups (Fig. 2; Fig.-e1, Supplemental Digital Content 5, <http://links.lww.com/CCM/F506> [legend, Supplemental Digital Content 8, <http://links.lww.com/CCM/F509>]; and Table e-3, Supplemental Digital Content 7,

<http://links.lww.com/CCM/F508>). With a single marker, the discrimination between traumatic and anoxo-ischemic patients was suboptimal for canonical ROIs (best marker RD in the cingulum AUC, 0.79; 95% CI, 0.78–0.80 and second best marker FA in the cingulum AUC, 0.72; 95% CI, 0.71–0.73). However, combining two subregions increased the AUC to 0.94 (95% CI, 0.93–0.95) (RD in the posterior cingulum combined with MD in the mPFC08). The SVC model resulted in an accuracy of 0.75 ( $p = 0.062$ ; FDR- $p = 0.062$ ). **Figure 3** shows the subregions leading to the best performance for group and etiology classification, together with the decision surface of the relevant model and the most selected features for discrimination.

### Prognostic Value

Using the mPFC–PMC connectivity we obtained predictions correlating with  $r = 0.67$  with the CRS-R measured 3 months after the MRI acquisition ( $ame = 3.7$ ). Using the same marker but a binary outcome variable we could obtain an AUC of

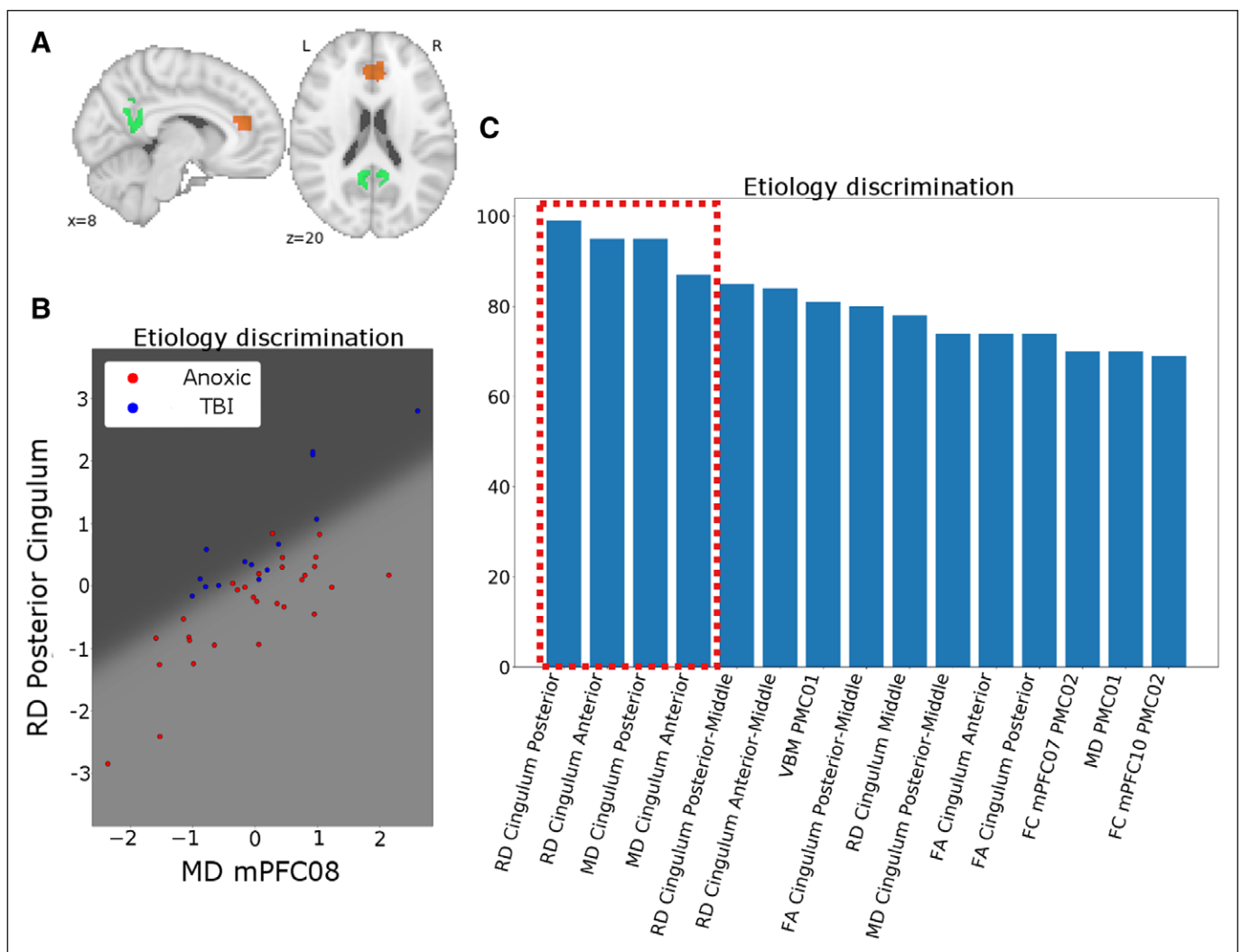


**Figure 3.** Discrimination: brain injury mechanism. **A**, Two indexes/regions of interests (ROIs) that led to the best etiology classification. Structural indexes (in this case radial diffusivity [RD] and mean diffusivity [MD]) are represented by a full colored ROI. **B**, Decision surface of the best model (logistic regression). **C**, Fifteen most selected features (out of 100 repetitions) in the model combining all features. Please note that the five most relevant features (*dashed red box*) are exclusively structural parameters. FC = functional connectivity, mPFC = medial prefrontal cortex, PMC = posteromedial cortex, TBI = traumatic brain injury, VBM = voxel-based morphometry.

0.89 (95% CI, 0.88–0.90). The performances increased when using the subregions, with the MD in the anterior cingulum being the best markers for CRS-R ( $r = 0.75$ ;  $\text{ame} = 3.1$ ) and the MD in the mPFC06 for the binary outcome (AUC, 0.91; 95% CI, 0.90–0.91). As for the combinations of subregions, the best combinations for predicting the CRS-R was the mPFC02–PMC01 connectivity with the PFC02–PMC02 connectivity ( $r = 0.78$ ;  $\text{ame} = 3.1$ ), while for the binary outcome the best combination was the mPFC01–PMC01 with the mPFC09–PMC02 connectivity (AUC, 0.96; 95% CI, 0.95–0.97). **Figure 4** shows the subregions leading to the best performance for outcome predictions (both as continuous CRS-R and binary as

favorable/unfavorable), together with the decision surface of the relevant models. When combining all indexes and using CRS-R as outcome variable we could reached an average correlation between predicted and measured CRS-R of  $r = 0.67$  ( $p = 0.06$ ;  $\text{FDR-}p = 0.062$ ), while using binary label we reached an accuracy of 0.81 ( $p = 0.02$ ;  $\text{FDR-}p = 0.04$ ). As shown in Figure 4 the most selected features for this pipeline were those relative to mPFC–PMC subregions FC. Importantly, there was an overlap between the features selected for both outcomes (CRS-R and binary), as well as between the features selected in this pipeline and those deemed most discriminative in the single and two markers analyses.

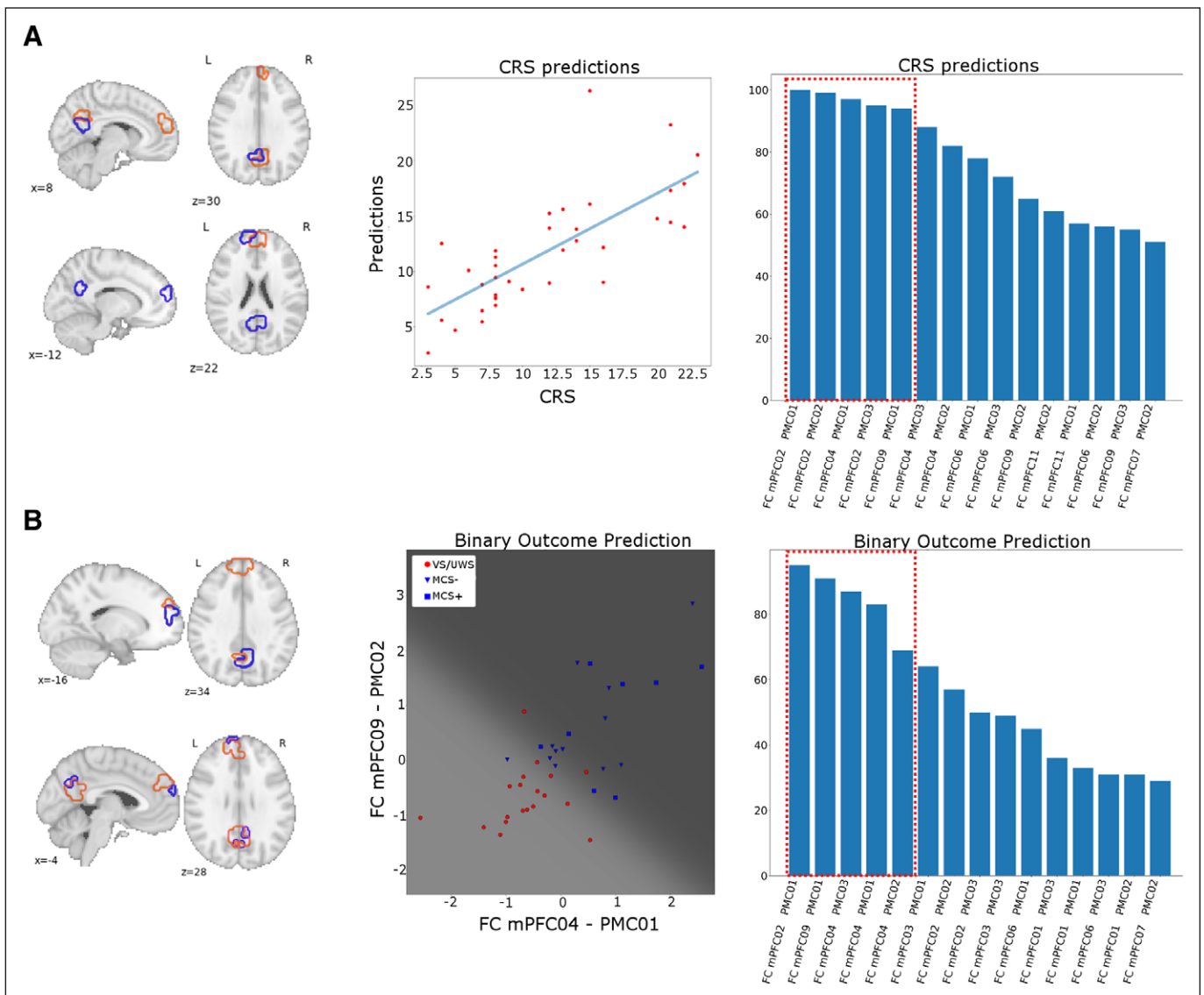


**Figure 4.** Prediction: neurologic outcome. **A, Leftmost** shows the two indexes/regions of interests (ROIs) that led to the best prediction of the outcome as measured by Coma Recovery Scale-Revised (CRS-R). Functional connectivity (FC) between two regions is represented using ROIs outline of the same color. **Central** shows the scatterplot of the relationship between CRS-R predictions obtained with the best model (linear regression) and actual CRS-R. **Rightmost** shows the most selected features (out of 100 repetitions) in the model combining all features (support vector regression). **B, Leftmost** shows the two indexes/ROIs that led to the best prediction of the binary outcome. FC between two regions is represented using ROIs outline of the same color. **Central** shows the decision surface of the best model (logistic regression), with the color reflecting the variable using for binary prediction: recovered (minimally conscious state [MCS]– and MCS+) in *blue* and not recovered (vegetative state [VS]/unresponsive wakefulness syndrome [UWS]) in *red*. The marker shape reflecting the specific 3 mo clinical status as VS/UWS (*circle*), MCS– (*triangle*), and MCS+ (*square*). **Rightmost** shows the most selected features (out of 100 repetitions) in the model combining all features. Please note that the five most relevant features (*red dashed box*) are FC parameters. mPFC = medial prefrontal cortex, PMC = posteromedial cortex.



## DISCUSSION

In this prospective study, coma patients had a significant functional disconnection between the mPFC and the PMC, irrespective of brain injury mechanism. This result is in line with previous rs-fMRI studies in coma studies and fits well with the empirical model of a “brain mesocircuit” (34), encompassing mPFC and PMC structures as a plausible candidate for the neural bases of DoC. As we hypothesized, early-acquired multimodal MRI data, permit to accurately predict coma patient’s 3-month outcome. It is worth noting the key role of functional data for the performance of our data-driven predictive model. In a clinical setting where MRI acquisition might be practically challenging to obtain, this result advocates for combining both functional and structural MRI techniques to improve the yield of a single MRI.

In line with experimental animal and human postmortem studies who have identified diffuse axonal injury as a key process underlying TBI patients cognitive impairment (27, 35), traumatic coma appeared to be strongly associated to massive cingulum damage. Coherently, significant white matter structural damage was observed across all DTI metrics (FA, MD, RD) and at the level of each cingulum segmentation. On the other hand, anoxo-ischemic coma patients had significant perturbation of the cortical microarchitecture, predominantly at the PMC. We suggest that this specific cortical structural disturbance, which we observed specifically in the anoxo-ischemic group might be related to the fact that PMC has one of the highest basal metabolic level within the brain (36) which make it intrinsically vulnerable to anoxo-ischemic insult. We suggest that this structural data might be useful to disentangle mixed primary and secondary brain insults, which are frequently observed in this setting (27, 37).

To the extent of our knowledge, there are not prior studies of the size of our study with acute advanced structural MRI and fMRI. One additional strength of our work was the limited impact of potential bias of self-fulfilling prophecies and the standardized MRI conditions acquisitions. Nevertheless, our study design is not without limitations: future and ongoing studies should focus on larger and longer longitudinal follow-up patients’ cohorts to specifically probe frontoparietal multimodal connectivity and the integrity of additional brain regions that putatively belong to the neural correlate of consciousness (e.g., ascending midbrain reticular activating system, thalamus). Furthermore, it should be acknowledged that the sample size limits the generalizability of our finding, especially concerning the discriminant and predictive models. However, it should be noted that our results were consistent relative to different statistical approaches (logistic regression and SVM) and fitting procedures (bootstrap and nested cross-validation). This strengthen the reliability of our findings.

In conclusion measuring the residual integrity of frontoparietal connections in coma patients by using a data-driven combination of structural MRI and fMRI measures appears to be an accurate tool to predict coma outcome at 3 months, as assessed by CRS-R. Patients with acute DoC have significantly lower levels of FC between the PMC and mPFC

than did controls. Structural MRI metrics—encompassing both gray and WM microstructural modifications—were not reliable biomarkers of coma per se but provide specific information about brain injury mechanism. Future studies should specifically address the implementation of such state-of-the-art neuroimaging tools to successfully built new personalized medicine approaches that will eventually permit to improve coma patient’s neurologic outcome.

## ACKNOWLEDGMENTS

We thank the technicians and engineers of Toulouse Neuro-Imaging Center (Helene Gros-Dagnac, Nathalie Vayssiere) and the medical and nurse staff of the Critical Care Units of the University Hospital of Toulouse for their active participation in coma neuroimaging studies.

Drs. Peran, Malagurski, Nemmi, and Sarton contributed equally to this article.

Supplemental digital content is available for this article. Direct URL citations appear in the printed text and are provided in the HTML and PDF versions of this article on the journal’s website (<http://journals.lww.com/ccmjournal>).

This work was supported by the “Association des Traumatisés du Crâne et de la Face”, “Institut des Sciences du Cerveau de Toulouse,” and grant from University Hospital of Toulouse.

Dr. Fourcade disclosed government work. Dr. Olivot received funding from Bristol Myers Squibb, Medtronic, and Pfizer. Dr. Naccache received support for article research from INSERM Sorbonne University ICM. The remaining authors have disclosed that they do not have any potential conflicts of interest.

For information regarding this article, E-mail: [silvastein@me.com](mailto:silvastein@me.com); [silva.s@chu-toulouse.fr](mailto:silva.s@chu-toulouse.fr)

## REFERENCES

- Shrestha GS, Suarez JJ, Hemphill JC III: Precision medicine in neurocritical care. *JAMA Neurol* 2018; 75:1463–1464
- Giacino JT, Fins JJ, Laureys S, et al: Disorders of consciousness after acquired brain injury: The state of the science. *Nat Rev Neurol* 2014; 10:99–114
- Achard S, Delon-Martin C, Vértes PE, et al: Hubs of brain functional networks are radically reorganized in comatose patients. *Proc Natl Acad Sci U S A* 2012; 109:20608–20613
- Di Perri C, Bahri MA, Amico E, et al: Neural correlates of consciousness in patients who have emerged from a minimally conscious state: A cross-sectional multimodal imaging study. *Lancet Neurol* 2016; 15:830–842
- Di Perri C, Bastianello S, Bartsch AJ, et al: Limbic hyperconnectivity in the vegetative state. *Neurology* 2013; 81:1417–1424
- Fernández-Espejo D, Soddu A, Cruse D, et al: A role for the default mode network in the bases of disorders of consciousness. *Ann Neurol* 2012; 72:335–343
- Hannawi Y, Lindquist MA, Caffo BS, et al: Resting brain activity in disorders of consciousness: A systematic review and meta-analysis. *Neurology* 2015; 84:1272–1280
- Laureys S, Faymonville ME, Luxen A, et al: Restoration of thalamo-cortical connectivity after recovery from persistent vegetative state. *Lancet* 2000; 355:1790–1791
- Monti MM, Rosenberg M, Fazio P, et al: Thalamo-frontal connectivity mediates top-down cognitive functions in disorders of consciousness. *Neurology* 2015; 84:167–173
- Qiu J: Probing islands of consciousness in the damaged brain. *Lancet Neurol* 2007; 6:946–947



11. Silva S, Alacoque X, Fourcade O, et al: Wakefulness and loss of awareness: Brain and brainstem interaction in the vegetative state. *Neurology* 2010; 74:313–320
12. Stender J, Gosseries O, Bruno MA, et al: Diagnostic precision of PET imaging and functional MRI in disorders of consciousness: A clinical validation study. *Lancet* 2014; 384:514–522
13. Vanhaudenhuyse A, Noirhomme Q, Tshibanda LJ, et al: Default network connectivity reflects the level of consciousness in non-communicative brain-damaged patients. *Brain* 2010; 133:161–171
14. Norton L, Hutchison RM, Young GB, et al: Disruptions of functional connectivity in the default mode network of comatose patients. *Neurology* 2012; 78:175–181
15. Silva S, de Pasquale F, Vuillaume C, et al: Disruption of posteromedial large-scale neural communication predicts recovery from coma. *Neurology* 2015; 85:2036–2044
16. Silva S, Peran P, Kerhuel L, et al: Brain gray matter MRI morphometry for neuroprognostication after cardiac arrest. *Crit Care Med* 2017; 45:e763–e771
17. Velly L, Perlberg V, Boulieu T, et al: MRI-COMA Investigators: Use of brain diffusion tensor imaging for the prediction of long-term neurological outcomes in patients after cardiac arrest: A multicentre, international, prospective, observational, cohort study. *Lancet Neurol* 2018; 17:317–326
18. Rosazza C, Andronache A, Sattin D, et al: Coma Research Center, Besta Institute: Multimodal study of default-mode network integrity in disorders of consciousness. *Ann Neurol* 2016; 79:841–853
19. Dehaene S, Changeux JP: Experimental and theoretical approaches to conscious processing. *Neuron* 2011; 70:200–227
20. Horowitz SG, Braun AR, Carr WS, et al: Decoupling of the brain's default mode network during deep sleep. *Proc Natl Acad Sci U S A* 2009; 106:11376–11381
21. Amico E, Gomez F, Di Perri C, et al: Posterior cingulate cortex-related co-activation patterns: A resting state fMRI study in propofol-induced loss of consciousness. *PLoS One* 2014; 9:e100012
22. Malagurski B, Péran P, Sarton B, et al: Neural signature of coma revealed by posteromedial cortex connection density analysis. *Neuroimage Clin* 2017; 15:315–324
23. Malagurski B, Péran P, Sarton B, et al: Topological disintegration of resting state functional connectomes in coma. *Neuroimage* 2019; 195:354–361
24. Threlkeld ZD, Bodien YG, Rosenthal ES, et al: Functional networks reemerge during recovery of consciousness after acute severe traumatic brain injury. *Cortex* 2018; 106:299–308
25. Giacino JT, Kalmar K, Whyte J: The JFK Coma Recovery Scale-Revised: Measurement characteristics and diagnostic utility. *Arch Phys Med Rehabil* 2004; 85:2020–2029
26. Rossetti AO, Rabinstein AA, Oddo M: Neurological prognostication of outcome in patients in coma after cardiac arrest. *Lancet Neurol* 2016; 15:597–609
27. Stocchetti N, Carbonara M, Citerio G, et al: Severe traumatic brain injury: Targeted management in the intensive care unit. *Lancet Neurol* 2017; 16:452–464
28. Teasdale G, Jennett B: Assessment of coma and impaired consciousness. A practical scale. *Lancet* 1974; 2:81–84
29. Wijdicks EF, Rabinstein AA, Bamlet WR, et al: FOUR score and Glasgow Coma Scale in predicting outcome of comatose patients: A pooled analysis. *Neurology* 2011; 77:84–85
30. Behrens TE, Woolrich MW, Jenkinson M, et al: Characterization and propagation of uncertainty in diffusion-weighted MR imaging. *Magn Reson Med* 2003; 50:1077–1088
31. Giacino JT, Ashwal S, Childs N, et al: The minimally conscious state: Definition and diagnostic criteria. *Neurology* 2002; 58:349–353
32. Giacino JT, Katz DI, Schiff ND, et al: Practice guideline update recommendations summary: Disorders of consciousness: Report of the Guideline Development, Dissemination, and Implementation Subcommittee of the American Academy of Neurology; the American Congress of Rehabilitation Medicine; and the National Institute on Disability, Independent Living, and Rehabilitation Research. *Neurology* 2018; 91:450–460
33. Giacino JT, Katz DI, Schiff ND, et al: Comprehensive systematic review update summary: Disorders of consciousness: Report of the Guideline Development, Dissemination, and Implementation Subcommittee of the American Academy of Neurology; the American Congress of Rehabilitation Medicine; and the National Institute on Disability, Independent Living, and Rehabilitation Research. *Neurology* 2018; 91:461–470
34. Schiff ND: Recovery of consciousness after brain injury: A mesocircuit hypothesis. *Trends Neurosci* 2010; 33:1–9
35. Maas AIR, Menon DK, Adelson PD, et al: InTBIIR Participants and Investigators: Traumatic brain injury: Integrated approaches to improve prevention, clinical care, and research. *Lancet Neurol* 2017; 16:987–1048
36. Hagmann P, Cammoun L, Gigandet X, et al: Mapping the structural core of human cerebral cortex. *PLoS Biol* 2008; 6:e159
37. Menon DK, Maas AI: Traumatic brain injury in 2014. Progress, failures and new approaches for TBI research. *Nat Rev Neurol* 2015; 11:71–72